# Common path optical coherence tomography using dual source by reducing autocorrelation noise for improved image quality

M. SHALABY*, F. S. ALORIFI, K. ALSNAIE
*Electrical Engineering Department, Faculty of Engineering, Al Imam Mohammad Ibn Saud Islamic University, Riyadh, KSA*

In this work, we present an improvement on the use of dual source in Optical Coherence Tomography measurement technique. In a common path configuration, we propose adding antireflection coating (AR-coating) layers to the fiber probe end which act only with wavelengths of one of the sources and not the other. The two sets of measurements are manipulated in such a way that autocorrelation noise is greatly reduced and image details are enhanced.

(Received June 7, 2018; accepted February 12, 2019)

*Keywords:* Optical Coherence Tomography (OCT), Coherent optical effects, Coherence imaging

## 1. Introduction

The use of optical Coherence Tomography OCT in human tissue imaging is increasing since its invention in 1990's [1,2]. OCT is a high-resolution imaging method, but OCT images experience some artifacts that lead to obscuring some tissue structures [2]. OCT image resolution and depth lies between ultrasonic and confocal microscopy. The OCT axial resolution reached 3 μm and its depth is around several millimeters. OCT setup implementation is categorized to two types; Time Domain TD-OCT, and Frequency Domain FD-OCT. TD-OCT makes use of a broad light source and comprises a moving mirror in the reference arm to determine the tissue layer which will be imaged. The measured signal represents directly the position of the layer and the reflected intensity produced from this layer. In this approach axial resolution varies directly with light source linewidth and depth of imaging varies inversely with mirror motion step size. In FD-OCT [5-12] the reference signal arises from a fixed mirror and is implemented in two ways, the first makes use also of a broad light source which is called Spectral Domain SD-OCT and the second employs a swept laser source with narrow linewidth which is called Swept Source SS-OCT. In SD-OCT, The measured signal is analyzed using an optical spectrum analyzer to get which we call an interferogram. Fourier transform of this interferogram produces tissue layers structure. Axial resolution in this technique depends on light source linewidth and depth of imaging varies inversely with the used OSA resolution. In SS-OCT, the measured signal versus source wavelength is in this case the interferogram to which Fourier transform should be applied to retrieve tissue layers structure. Axial resolution in this approach varies directly with laser swept range whereas depth of imaging varies inversely with minimum change in swept laser source wavelength.

Due to the high imaging speed, FDOCT systems [3,4] enable the acquisition of three dimensional image data *in-vivo* which is especially beneficial for numerous ophthalmic imaging applications [6,13].

Despite its superiority over TDOCT, FDOCT implementation exhibits drawbacks in terms of autocorrelation noise artifacts, which obscures details of the image and degrades the system performance. The autocorrelation terms arise from the interference occurring between different sample reflectors within the target. Jun Ai, et al. proposed the elimination of autocorrelation noise through asynchronous acquisition of two interferograms using an optical switch and attaining an axial resolution of 15 μm in air [14].

Autocorrelation noise reduction was proposed by Shalaby, et al. [18], using a concept of resonance between tissue layers and a laser cavity instead of using an external light source. In this paper we propose the use of a dual light source at two different center wavelengths in a common path FD-OCT. The tip of the fiber probe is coated with dielectric layers such as to eliminate the reference signal produced from the fiber tip at wavelengths of the first light source. In this case, the interferogram obtained from the first light source represents only the autocorrelation noise. The interferogram obtained from the second light source represents the tissue layers in addition to autocorrelation noise. Special treatment of the two interferograms taking into consideration difference in tissue dispersion at the two wavelengths of the used sources results in an image with great reduction of autocorrelation noise.

## 2. Analysis

FD-OCT is based on low coherence interferometry. The main concept of OCT is the same as that of the simple Michelson interferometer except that one of its mirrors is replaced by the sample under investigation. Axial (depth) resolution "ΔL" is inversely proportional to light bandwidth. The advantage of increased resolution is lost by the autocorrelation noise that covers required signals of the sample structure.

The employment of two light sources in order to get a higher bandwidth and hence a better resolution was proposed by Tarek, [15], where he concluded that using two sources with two separate spectra does not necessarily leads to improved resolution.

In this paper, we present a novel implementation of a common path OCT setup that is free from the autocorrelation noise signals that may overlap the desired image of the object layers. This is achieved through the employment of two light sources instead of a single source. In the common path OCT configuration, adopted in our work, the end of the fiber probe used is prepared with coating dielectric layers. These coating layers eliminate reflection off fiber end at wavelengths of one of the used light sources and not the other. The idea behind the proposed system is to acquire two interferograms each caused by one of the light sources. The interferogram caused without reflection of the fiber end represent autocorrelation noise. This interferogram is shifted towards the same wavelengths of the second source taking into consideration both sample dispersion, and difference between the two sources regarding their intensities and linewidths. The shifted interferogram is then subtracted from the second interferogram. Fourier transform of the resulting interferogram gives the detailed structure of the sample layers and shows a great reduction in autocorrelation noise. The obtained image details, due to the absence of undesired signals, shows an enhancement over the OCT technique employing a single source.

## 3. Experimental setup of dual source OCT technique

Fig. 1 shows the experimental setup we studied in our proposed system. The end of the used fiber probe is coated with antireflection dielectric layers (AR-coating) acting with wavelength range of SLD-1 and hence, the reference signal is absent at this wavelength range. Let the interferogram obtained in this case be called $I_1(\lambda)$. At the other wavelength range of SLD-2, the effect of AR-coating disappears and hence there is a reference signal reflected off the fiber end. Let the interferogram obtained at this wavelength range be called $I_2(\lambda)$. The idea of the algorithm used is summarized as follows:

1- The envelopes of the emitted intensity versus wavelength of each LED source, $S_1(\lambda)$ and $S_2(\lambda)$, are captured and saved for the normalization process required at the step of cancelling autocorrelation noise.

2- Fast Fourier Transform FFT is applied on the first interferogram $I_1(\lambda)$ to produce a structure of tissue layers representing the autocorrelation noise since the reference signal is absent.

3- This structure of layers is then used to produce an interferogram at the wavelength range of the second LED source. At this step, tissues dispersion is taken into consideration. Let the translated interferogram be called $I_t(\lambda)$.

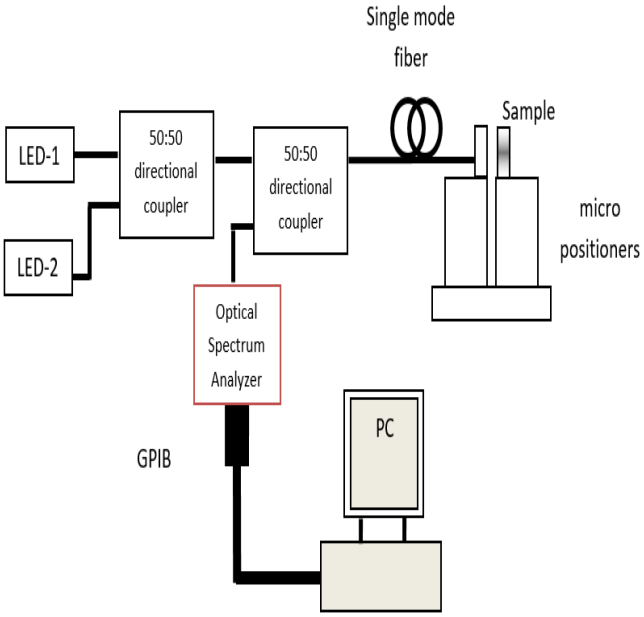


*Fig. 1. Experimental setup used to examine the proposed Dual Source Optical Coherence Tomography technique*

4- At this step, the envelopes of the two light sources saved before are used to normalize $I_t(\lambda)$ and $I_2(\lambda)$, producing $I_t'(\lambda)$ and $I_2'(\lambda)$.

5- The translated interferogram obtained $I_t'(\lambda)$ is then subtracted from the second interferogram at the wavelength range of the second SLD source $I_2'(\lambda)$. We call the result of subtraction $I_d(\lambda)$.

6- FFT is then applied on $I_d(\lambda)$ to get a better and clear image of the actual tissues structure since it is free from autocorrelation noise. Therefore, we can profit from the increased resolution of this imaging technique.

## 4. Dispersion in OCT systems

Dispersion in OCT causes degradation in system performance where reflected signals of sample layers suffer broadening which leads toward loss of axial resolution. Dispersion is introduced through a Taylor series expansion of the propagation constant k as;

$$k(\omega) = k(\omega_o) + (\omega - \omega_o)\frac{\partial k}{\partial \omega} + \frac{1}{2}(\omega - \omega_o)^2 \frac{\partial^2 k}{\partial \omega^2} + \frac{1}{6}(\omega - \omega_o)^3 \frac{\partial^3 k}{\partial \omega^3} + \cdots. \quad (1)$$

The third term represents first order dispersion or group velocity dispersion, and the fourth term represents second order dispersion. Tissues material is the origin of this dispersion.

To examine the effect of refractive index dispersion we adopted Cauchy dispersion equation of the refractive index of layered skin tissues [15, 16] as;

$$n_r = A + \frac{B}{\lambda^2} + \frac{C}{\lambda^4} \quad (2)$$

The coefficients are given as:

$$\begin{bmatrix} A \\ B \\ C \end{bmatrix} = \begin{bmatrix} 1.3696 \\ 3.9168 \times 10^3 \\ 2.5588 \times 10^3 \end{bmatrix} \quad (3)$$

where wavelengths are in nanometers.

## 5. Simulation results

A sample of predetermined shape is assumed in our analysis to test the validity of our new algorithm. A sample having four layers positioned at 0.5, 0.7, 1.125, and 1.5 mm is considered. The interferogram resulting from this sample structure, for each light source, is calculated using the relation [17];

$$I(\lambda) = S(\lambda) \sum_{i=0}^{N} \rho_i \cos\left(\frac{4\pi}{\lambda} \sum_{t=0}^{i} n_t \, d_t\right) \quad (4)$$

where N is the total number of studied layers, $\rho_i$ is the reduced amplitude reflectivity of each layer, and $n_t$, and $d_t$ represent refractive index and thickness of the $t^{th}$ layer.

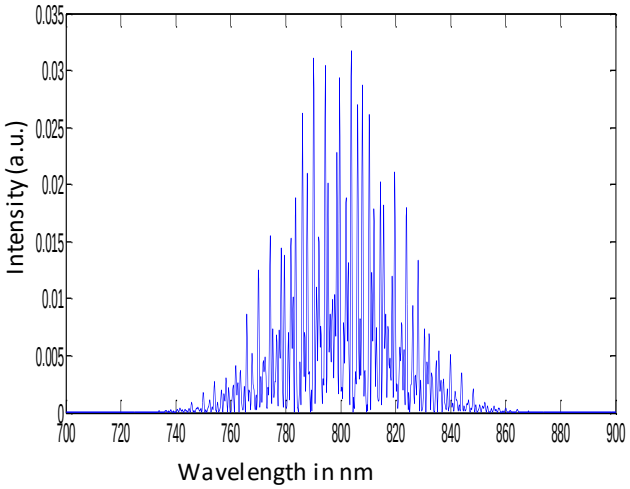


*Fig. 2. Interferogram $I_1(\lambda)$ produced by the first light source*

Figs. 2, 3 show the interferograms captured by the first light source centered at 0.8 μm and the second light source centered at 1.3 μm respectively. Figs. 4, 5 show the FFT of the interferograms displayed in Figs. 2, 3 respectively. Fig. 4 represents autocorrelation noise arising due interference between different sample layers. Fig. 5 shows sample layers along with those of Fig. 4. Finally Fig. 6 shows sample layers after applying our previously explained algorithm. Layers shown in this figure correspond only to interference occurring between signals reflected of tissue layers in one hand and the reference signal in the other hand.

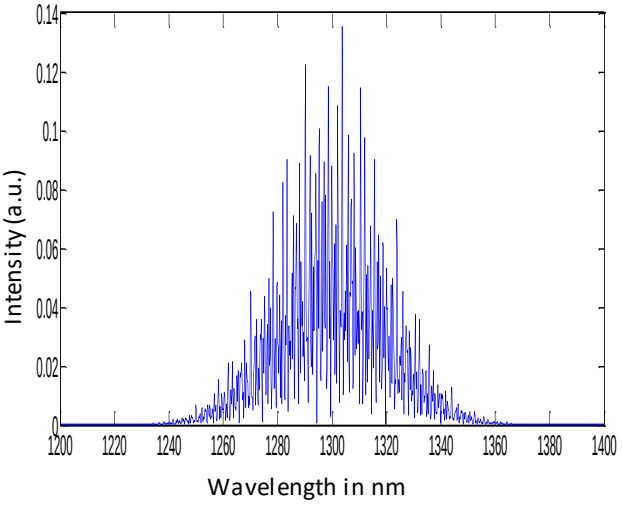


*Fig. 3. Interferogram $I_2(\lambda)$ produced by the second light source*

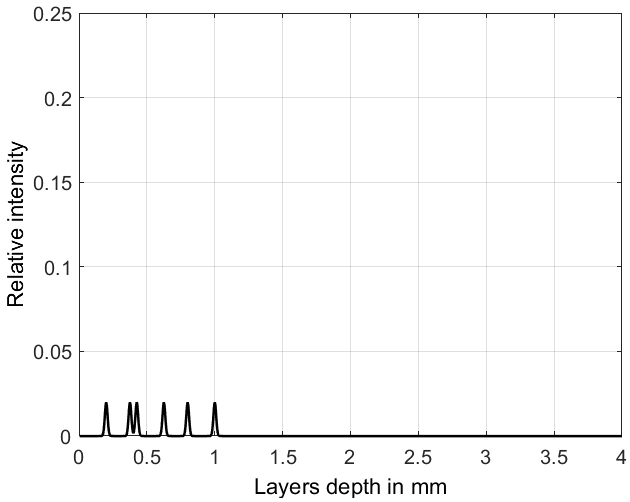


*Fig. 4. Autocorrelation noise alone, which is the Fourier transform of the first interferogram*

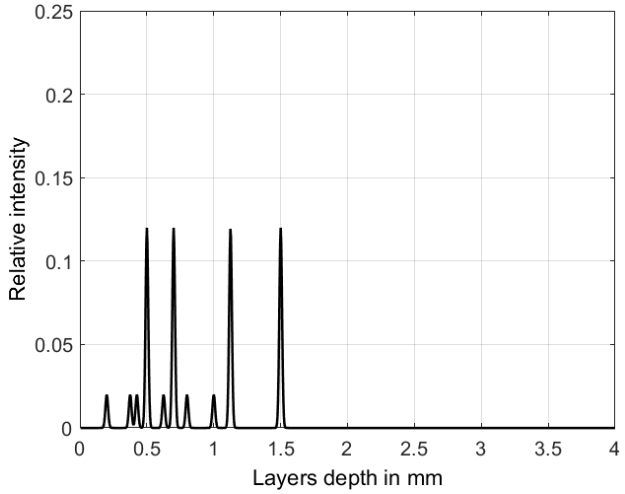


*Fig. 5. The Fourier transform of the second interferogram*

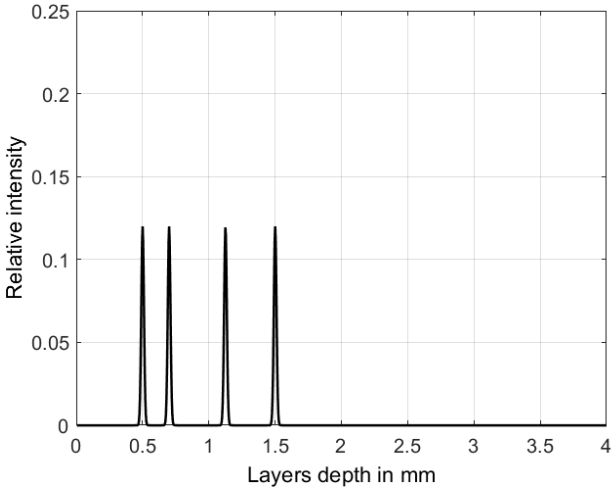


*Fig. 6. Noise free image of sample layers*

## 6. Experimental results

In what follows we show the results of our proposed experimental setup compared to the same results obtained using a conventional common path FD-OCT.

The studied sample is a glass microscope slide of thickness 1.1 mm approximately. The light sources used have bandwidth of approximately 60 nm centered at 1300 and 1550 nm. The Agilent Optical Spectrum Analyzer used has a spectral resolution of 0.07 nm. We apply Fast Fourier Transform for both interferograms to attain the detailed layers structure of the studied sample as explained before.

Fig. 7a shows the layers positions and levels obtained using the ordinary OCT algorithm using only one light source. Coherence noise term is expected to appear at the position of 1.1 mm (the glass sheet thickness). The signal level at this position is about one third the level of the original signal corresponding to the second surface of the tested sample. Fig. 7b shows the results obtained for the same sample using dual light sources and applying the new algorithm. The signal level at the position of the autocorrelation noise is very weak about one tenth the original signal of the second surface. This emphasizes our expectation of getting a much reduced coherence noise. The overall reduction in autocorrelation noise signal level is nearly 5dB.

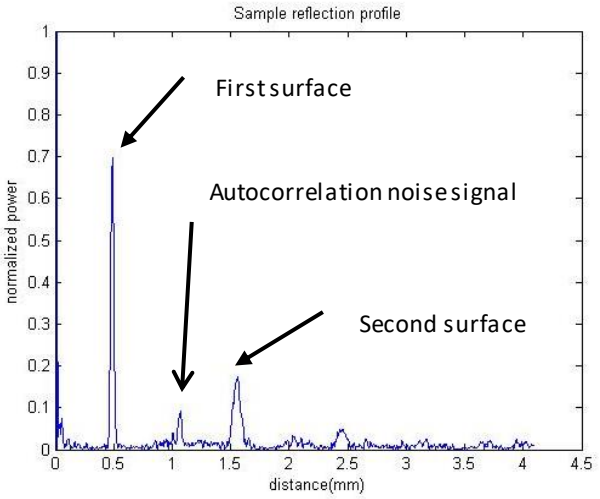


*Fig. 7a. Layers positions of the glass sheet when measured using the ordinary OCT method showing the relatively high level of the autocorrelation noise signal*

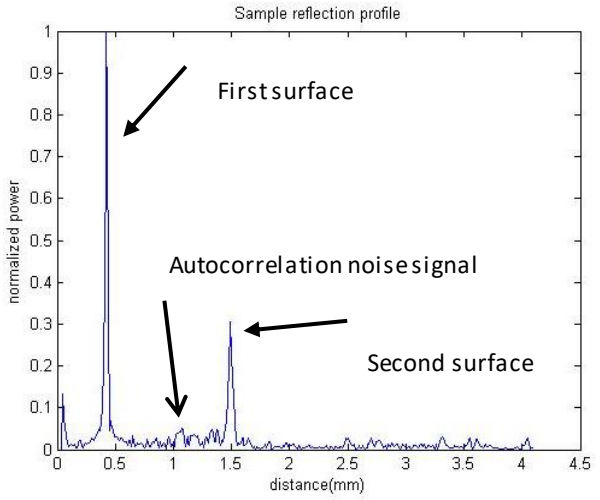


*Fig. 7b. Layers positions of the same sample as Fig. 7a, measured using the Dual Source OCT method showing the autocorrelation noise signal highly reduced*

## 7. Conclusion

We presented in this work a method to eliminate -to a great extent- the autocorrelation noise inherent in OCT imaging technique. The results obtained show that image details masked by this type of noise became clear and easier to visualize. Hence, the technique became more appropriate to analyze human tissue structures to get more accurate diagnosis and distinguish between healthy and

unhealthy cases. The cost paid for this increased clarity of image details is that of the added second set of measurements at the other wavelength range of the additional LED source.

**Acknowledgments**

The authors would like to thank the Deanship of Scientific Research at Al Imam Mohammad Ibn Saud Islamic University, Saudi Arabia for financing this project under the grant no. (381404), and for the continuous help during this work by providing the space and equipment required to carry out the experimental measurements.

## References

[1] D. Huang, E. A. Swanson, C. P. Lin, J. S. Schuman, W. G. Stinson, W. Chang, M. R. Hee, T. Flotte, K. Gregory, C. A. Puliafito, J. G. Fujimoto, Science **254**, 1178 (1991).
[2] Saba Adabi, Zahra Turani, Emad Fatemizadeh, Anne Clayton, Mohammadreza Nasiriavanaki, Biomedical Engineering and Computational Biology **8**, 1 (2017).
[3] R. Leitgeb, C. K. Hitzenberger, A. F. Fercher, Opt. Express **11**, 889 (2003).
[4] J. F. de Boer, B. Cense, B. H. Park, M. C. Pierce, G. J. Tearney, B. E. Bouma, Opt. Letters **28**, 2067 (2003).
[5] Zhenguo Wang, Zhijia Yuan, Hongyu Wang, Yingtian Pan, Opt. Express **14**(16), 7014 (2006).
[6] M. Wojtkowski, R. Leitgeb, A. Kowalczyk, T. Bajraszewski, A. F. Fercher, J. Biomed. Opt. **7**, 457 (2002).
[7] M. Wojtkowski, V. J. Srinivasan, T. H. Ko, J. G. Fujimoto, A. Kowalczyk, J. S. Duker, Opt. Express **12**, 2404 (2004).
[8] N. A. Nassif, B. Cense, B. H. Park, M. C. Pierce, S. H. Yun, B. E. Bouma, G. J. Tearney, T. C. Chen, J. F. de Boer, Opt. Express **12** (3), 367 (2004).
[9] S. R. Chinn, E. A. Swanson, J. G. Fujimoto, Opt. Lett. **22**, 340 (1997).
[10] F. Lexer, C. K. Hitzenberger, A. F. Fercher, M. Kulhavy, Appl. Opt. **36**, 6548 (1997).
[11] M. A. Choma, M. V. Sarunic, C. H. Yang, J. A. Izatt, Opt. Express **11**, 2183 (2003).
[12] S. H. Yun, G. J. Tearney, J. F. de Boer, B. E. Bouma, Opt. Express **12**, 5614 (2004).
[13] B. Cense, N. A. Nassif, T. C. Chen, M. C. Pierce, S.-H. Yun, B. H. Park, B. E. Bouma, G. J. Tearney, J. F. de Boer, Opt. Express **12**, 2435 (2004).
[14] Jun Ai, L. V. Wang, Applied Physics Letters **88**, 111115 (2006).
[15] M. J. Van Gemert, S. L. Jacques, H. J. Sterenborg, W. M. Star, IEEE Trans. Biomed. Eng. **36**, 1146 (1989).
[16] L. Wang, S. L. Jacques, L. Zheng, Comput. Methods Prog. Biomed. **47**, 31 (1995).
[17] Tarek A. AlSaeed, Mohamed Y. Shalaby, Diaa A. Khalil, Optical Engineering **54**(10), 104112 (2015).
[18] M. Shalaby, Sulaiman S. Al-Sowayan, Journal of the European Optical Society-Rapid Publications **12:10** (2016).

*Corresponding author: mshalaby88@gmail.com